CARDIAC

Optimizing radiation dose by using advanced modelled iterative reconstruction in high-pitch coronary CT angiography

Sonja Gordic[1] · Lotus Desbiolles[1,2] · Martin Sedlmair[3] ·
Robert Manka[1,4,5] · André Plass[6] · Bernhard Schmidt[3] ·
Daniela B. Husarik[1] · Francesco Maisano[6] ·
Simon Wildermuth[2] · Hatem Alkadhi[1] ·
Sebastian Leschka[1,2]

Abstract

Purpose To evaluate the potential of advanced modeled iterative reconstruction (ADMIRE) for optimizing radiation dose of high-pitch coronary CT angiography (CCTA).

Methods High-pitch 192-slice dual-source CCTA was performed in 25 patients (group 1) according to standard settings (ref. 100 kVp, ref. 270 mAs/rot). Images were reconstructed with filtered back projection (FBP) and ADMIRE (strength levels 1–5). In another 25 patients (group 2), high-pitch CCTA protocol parameters were adapted according to results from group 1 (ref. 160 mAs/rot), and images were reconstructed with ADMIRE level 4. In ten patients of group 1, vessel sharpness using full width at half maximum (FWHM) analysis was determined. Image quality was assessed by two independent, blinded readers.

Results Interobserver agreements for attenuation and noise were excellent ($r=0.88/0.85$, $p<0.01$). In group 1, ADMIRE level 4 images were most often selected (84 %, 21/25) as preferred data set; at this level noise reduction was 40 % compared to FBP. Vessel borders showed increasing sharpness (FWHM) at increasing ADMIRE levels ($p<0.05$). Image quality in group 2 was similar to that of group 1 at ADMIRE levels 2–3. Radiation dose in group 2 (0.3 ± 0.1 mSv) was significantly lower than in group 1 (0.5 ± 0.3 mSv; $p<0.05$).

Conclusions In a selected population, ADMIRE can be used for optimizing high-pitch CCTA to an effective dose of 0.3 mSv.

Key points

• *Advanced modeled IR (ADMIRE) reduces image noise up to 50% as compared to FBP.*
• *Coronary artery vessel borders show an increasing sharpness at higher ADMIRE levels.*
• *High-pitch CCTA with ADMIRE is possible at a radiation dose of 0.3 mSv.*

Keywords Computed tomography · Radiation dose · Iterative reconstruction · Coronary angiography · Image quality

✉ Hatem Alkadhi
hatem.alkadhi@usz.ch

1   Institute of Diagnostic and Interventional Radiology, University Hospital Zurich, University of Zurich, Raemistrasse 100, CH-8091 Zurich, Switzerland

2   Divison of Radiology and Nuclear Medicine, Kantonsspital, St. Gallen, Switzerland

3   Siemens Healthcare, Computed Tomography Division, Forchheim, Germany

4   Clinic of Cardiology, University Hospital Zurich, University of Zurich, Zurich, Switzerland

5   Institute for Biomedical Engineering, University and ETH Zurich, Zurich, Switzerland

6   Clinic for Cardiovascular Surgery, University Hospital Zurich, University of Zurich, Zurich, Switzerland

Introduction

Optimizing radiation dose of coronary computed tomography angiography (CCTA) represents a permanent endeavour [1]. Many radiation dose reduction techniques were developed including adaptation of tube voltage [2], iterative reconstruction (IR) [3] and high-pitch scanning [4].

The recently introduced third-generation dual-source 192-slice CT provides a high-pitch scan mode allowing for prospective electrocardiography (ECG)-gated CCTA at heart rates up to 75 beats per minute (bpm) [5, 6]. This scanner also introduced a new IR technique, i.e. advanced modeled IR (ADMIRE) [7], representing the successor of the previous sinogram-affirmed IR (SAFIRE) algorithm. ADMIRE represents a hybrid IR technique and—compared with SAFIRE—includes into the analysis not only the nearest but also larger neighbourhood data [8]. ADMIRE uses a weighted-FBP algorithm accelerating the removal of geometrical imperfections, and noise is reduced owing to an interaction between statistical modelling in the raw and the image domain [7]. In contrast to conventional filtered back projection (FBP) reconstructions, IR algorithms permit a decoupling of spatial resolution and noise [9, 10], allowing for radiation dose reduction in CT imaging.

Previous studies evaluated high-pitch CCTA in regards to the maximally required heart rate [5, 6] and to optimal tube voltage levels and contrast media dosages [4]. However, no study so far—to the best of our knowledge—investigated the potential of ADMIRE for improving the dose efficiency of high-pitch CCTA, which was the purpose of this study. For this, we subdivided our patients into two groups: In the first group we evaluated the quantitative and qualitative image quality achieved with ADMIRE at different strength levels, and in the second group we applied the results from the first group in a separate patient population to demonstrate the potential for radiation dose reduction of ADMIRE in high-pitch CCTA.

Materials and methods

Study population

The present retrospective study was conducted after institutional review board approval was obtained. Written informed consent was waived by the local ethics committee because all CT examinations were clinically indicated, and no CT examination was performed for the mere purpose of the study.

In total, 50 consecutive patients (13 female, median age 54 years, age range 39–82 years) undergoing clinically indicated CCTA were included. All patients were referred to CCTA for evaluation of suspected coronary artery disease, had a low to intermediate risk of coronary artery disease and suffered from atypical chest pain. The indications were in accordance with current guidelines and recommendations [11]. Patients were included if their ECG after nitrate application indicated a heart rate (HR) no greater than 75 beats per minute (bpm). No beta-blockers were used. Exclusion criteria were impaired renal function (estimated glomerular filtration rate less than 30 ml/min), known hypersensitivity to iodinated

contrast material, pregnancy and an HR prior to the scan greater than 75 bpm and/or an irregular HR (Table 1).

This single-centre study included two groups constituting two patient populations, as previously shown [9, 12]. The aim of the first part of the study was to evaluate the effect of ADMIRE on qualitative and quantitative image quality in CCTA, whereas the aim of the second part was the application of the results from the first part in a separate patient population. In the first 25 patients (hereafter referred to as group 1), high-pitch CCTA was performed according to institutional standard CT protocol settings; the other 25 consecutive patients (hereafter referred to as group 2) were imaged with CT parameters resulting in a lower radiation dose being adapted from the results of group 1 (see "Results" section).

CT data acquisition

All scans ranged from the level of the tracheal bifurcation to the diaphragm. Each patient received a single oral dose of 2.5 mg isosorbiddinitrate sublingually (Isoket, Schwarz Pharma, Manheim, Germany) 2–3 min prior to the CCTA scan. An average of 60 ml (range 42–90 ml) contrast media (iopromide, Ultravist® 370, 370 mg iodine/ml, Bayer Schering Pharma, Berlin, Germany) was injected in an antecubital vein, followed by a chaser of 30 ml of diluted contrast media (20 % vol) with a dual-head power injector (Stellant®, Medrad, Inianola, USA) at a flow rate of 5.0–6.0 ml/s. Scan initiation was controlled by bolus tracking with a region of interest (ROI) in the ascending aorta, using a signal attenuation threshold of 120 Hounsfield units (HU) at 120 kVp. The scan delay was 10 s. Scans were performed with a 192-slice dual-source CT scanner (SOMATOM Force, Siemens Healthcare) equipped with a high resolution detector (Stellar Technology, Siemens) [13].

A protocol with prospective ECG-gating during one heart cycle with the data acquisition starting at 60 % of the R–R interval was chosen. Automated attenuation-based tube voltage selection (CAREkV, Siemens) with a reference tube voltage of 100 kVp was used. In addition, automated attenuation-based tube current modulation (CAREDose, Siemens) was applied. In group 1, the reference tube current–time product was 270 mAs/rotation (according to the institutional standard protocol). In group 2 the tube current–time product was set to 160 mAs/rotation (according to the results from group 1, see below).

Data reconstruction

Data were reconstructed with a field-of-view (FoV) of 200 mm, pixel matrix of 512×512, a medium-soft tissue kernel (Bv40), slice thickness of 0.6 mm and increment of 0.4 mm. In group 1, reconstructions were performed using FBP and with ADMIRE at strength levels of 1–5 (Fig. 1). In

Table 1 Patient characteristics, imaging parameters, and radiation dose parameters

	Group 1	Group 2	p value
No. of patients	25	25	–
Median age (range) [years]	50 (40–82)	56 (39–82)	NS
Female sex	24 % (6/25)	28 % (7/25)	NS
Mean heart rate (range) [bpm]	59±6	61±5	NS
Body mass index [kg/m^2]	24.9±2.8	25.3±3.4	NS
Tube voltage (range) [kVp]	88±12 (70–120)	82±8 (70–90)	NS
Tube current–time product (range) [mAs]	442±94 (257–648)	418±79 (322–573)	<0.05
Scan length (range) [mm]	122±6 (114–138)	126±11 (110–144)	NS
CTDI$_{vol}$ (range) [mGy cm]	3.0±1.6 (1.5–8.3)	2.1±0.7 (1.3–3.3)	<0.05
DLP (range) [mGy cm^{-1}]	37±19 (18–103)	26±9 (17–42)	<0.05
Radiation dose estimate (range) [mSv]	0.5±0.3 (0.3–1.4)	0.3±0.1 (0.2–0.6)	<0.05
SSDE [mGy]	1.9±1.0 (1.0–5.1)	1.4±0.4 (0.8–2.2)	<0.05
Contrast material (range) [ml]	62±13 (42–90)	58±9 (42–70)	NS

CNR contrast-to-noise ratio, *CTDI$_{vo}$* CT volume dose index, *DLP* dose–length product, *NS* not significant, *SSDE* size-specific dose estimates

group 2, reconstructions were performed with ADMIRE at a strength level of 4 (according to the results from group 1, see below).

ADMIRE includes statistical modelling in the raw data domain, followed by back projection, regularization in the image domain, and forward projection employing an adequate system model. The resulting pseudo-raw data are subtracted from the measurement data and are reinserted into the loop afterwards. ADMIRE uses a weighted-FBP in the loop. Mathematically this corresponds to a pre-conditioning filter, which accelerates the removal of non-exact reconstruction operators (i.e. non-iterative FBP) and geometric imperfections (i.e.

cone-beam artefacts). Noise is reduced owing to the interaction between statistical modelling in the raw data and in the image domain ("master 3D volume") [7].

CT data analysis

Qualitative analysis

Two independent radiologists (both with more than 10 years of experience in cardiovascular imaging) assessed all CCTA data sets in randomized order in regard to the IR-related image appearance including the texture naturalness but neglecting

Fig. 1 Examples of image quality with FBP and ADMIRE strength level 1 to 5. Note the only minor blotchy pixelated appearance of the anatomic structures in data sets reconstructed with ADMIRE at a strength level of 5
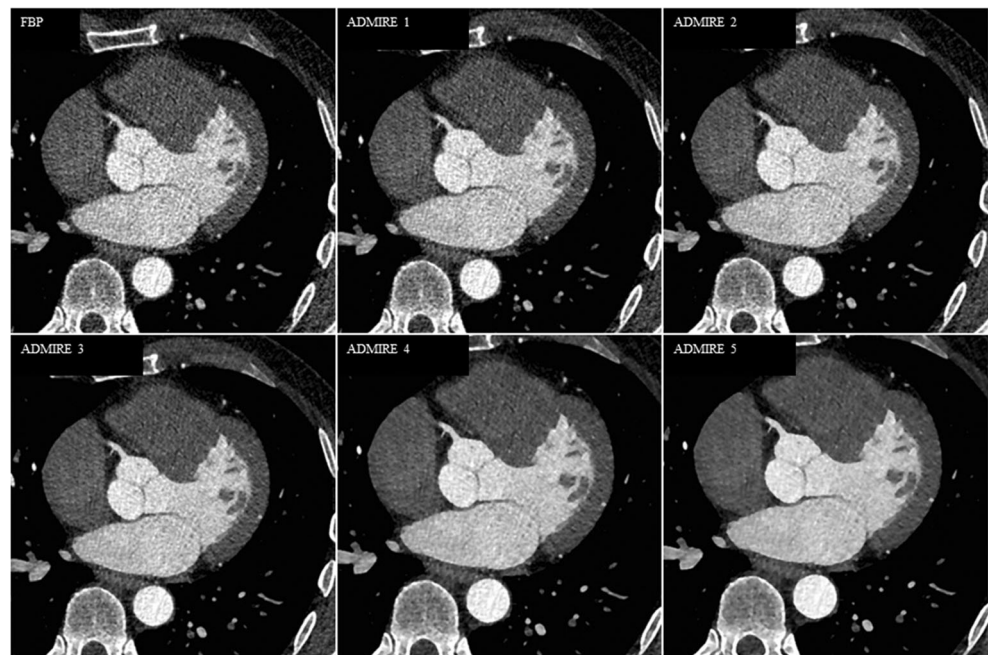
possible motion artefacts (because the focus of this study was radiation dose and image quality but not heart rate and motion artefacts). All coronary artery segments were analysed. The following scoring system was used as previously published [14]: score 1 indicated excellent image impression with a lack of plastic-like appearance; score 2 indicated good image appearance with minimal plastic-like appearance; score 3 indicated fair image appearance with moderate plastic-like appearance; and score 4 indicated poor image appearance with marked plastic-like appearance.

Graininess was assessed by both observers using a four-point Likert scale: score 1 indicated excellent image quality with minimal or no appreciable mottle; score 2 indicated good image quality with low image noise not interfering with the depiction of small coronary artery segments; score 3 indicated fair image quality with average graininess with satisfactory depiction of small coronary artery segments; and score 4 indicated poor image quality with unacceptable interference with the depiction of these structures.

Streak artefacts were defined as dark streaks adjacent to calcified coronary deposits, iodinated contrast, or other high-attenuation structures. Both observers assessed the presence of streak artefacts in all data sets using a three-point score: 1, streak artefacts absent; 2, streak artefacts present but not interfering with depiction of adjacent structures; 3, streak artefacts present and interfering with depiction of adjacent structures.

In addition, those image data sets in group 1 which were preferred for making the diagnosis were selected for each patient in consensus by the same two readers in all data sets (FBP, ADMIRE strength 1–5). The noise reduction of that data set selected relative to the noise level of FBP was used as a measure for the tube current reduction in group 2.

Individual adjustment of window centre and window width level settings was allowed.

Image sharpness evaluation

Image sharpness was measured in the first 10 patients of group 1 with the use of a custom-written image viewing and analysis software (ViSi version 1.0; Siemens Healthcare, Forchheim, Germany) by a third, independent reader. In each of the 10 patients and in each reconstructed data set, a line (length range 10–17 mm) was drawn perpendicular to the left main coronary artery (LMA, Fig. 2a) and in the proximal posterior descending artery (PDA) to include representative proximal and distal coronary segments in the vessel sharpness analysis. All pixel intensities along the lines were evaluated, and minimum and maximum intensity values were derived. The non-interpolated HU values along the line gave rise to a signal intensity profile for each data set. These signal intensity profiles were subsequently analysed visually by the two readers mentioned above in consensus, by determining the data set with the highest

sharpness within each patient visually (Fig. 2b–g). Then, the mean of the minimum and maximum was taken to calculate the location on the two legs of the trapezoid and the full width at half maximum (FWHM) was derived by measuring the distance between the two leg points. As a matter of fact, the slope of a leg and thus the area under the curve describe the sharpness mathematically using different reconstruction kernels and methods, disregarding contrast-to-noise influences [15]. In our setting with high contrast-to-noise ratios (CNR) the effect can be neglected, but has to be taken into account when measuring in low-contrast/high-noise conditions.

Coronary artery stenosis assessment

The one reader performing the image sharpness evaluation additionally assessed all coronary segments in both groups for the presence of substantial coronary artery stenosis, defined as luminal diameter narrowing exceeding 50 %.
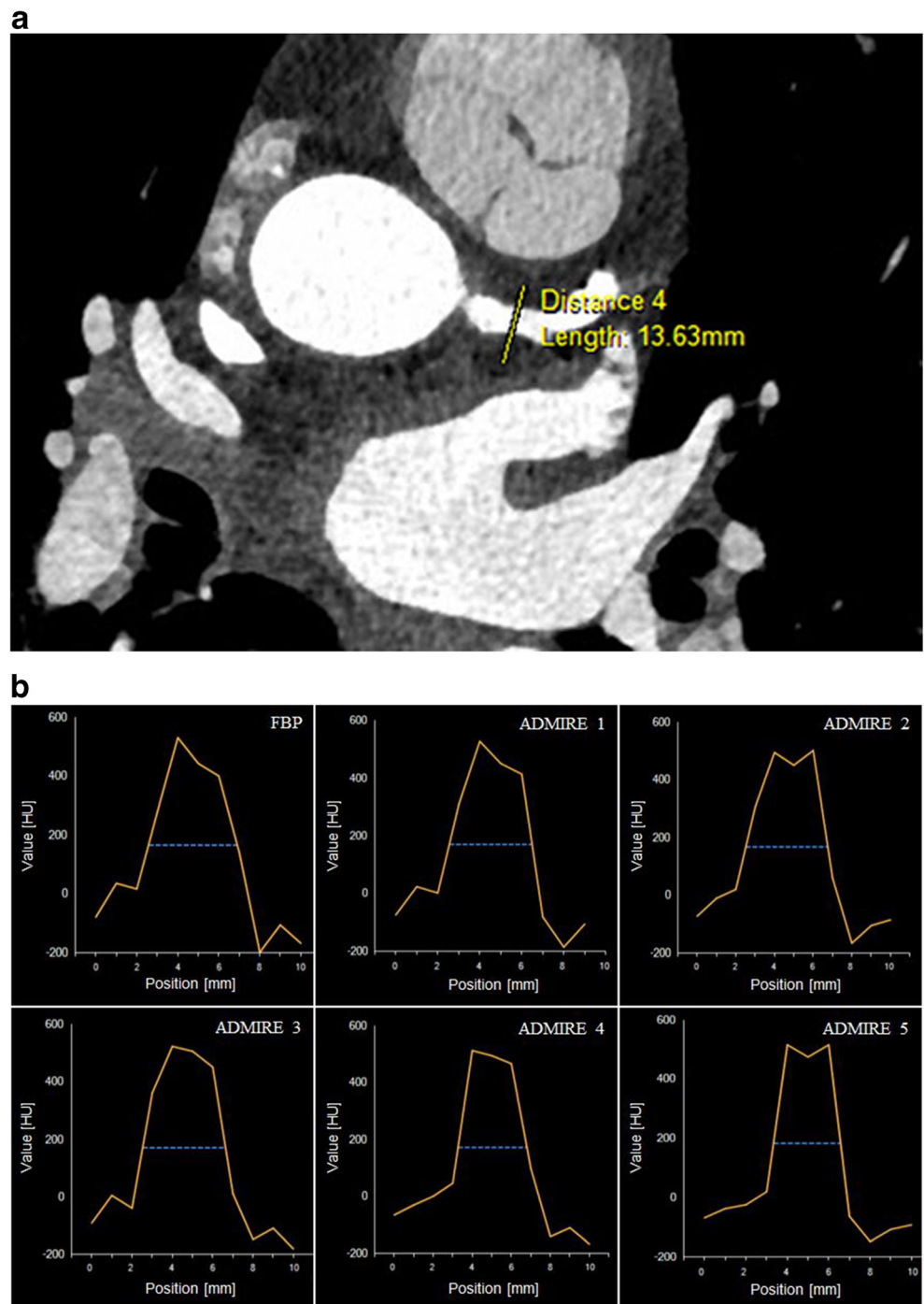
Quantitative analysis

Attenuation and noise were measured by two other independent observers. Calculations of the CNR in the aorta were performed as follows: First, attenuation was calculated as the difference in the mean attenuation (in HU) between the aorta at the level of the left main artery and the attenuation in the epicardial fat tissue on the same image. Attenuation in the ascending aorta was measured by placing a region of interest (ROI) of predefined size (1 cm^2) avoiding calcifications and plaques. Second, image noise was determined as the standard deviation of attenuation in the ROI in the aorta. Third, the CNR was calculated as the difference of attenuation in the ascending aorta divided by the noise. Measurements were performed twice by each observer and the average of both measurements was used for further analysis.

Estimation of the CT radiation dose

For an estimation of the radiation dose, the CT volume dose index (CTDI$_{vol}$) and the dose–length product (DLP) were taken from the electronically logged patient protocol. The scan length in the z-axis was calculated from the table position of the images. The effective dose of CCTA was derived from the product of the DLP and a conversion coefficient for the chest according to a method proposed by the European Working Group for Guidelines on Quality Criteria in CT [16]. A conversion coefficient of $k = 0.014$ mSv mGy^{-1} cm^{-1} was applied [16, 17].

Additionally size-specific dose estimates (SSDE) were calculated by using the conversion factors for effective diameters from the American Association of Physicists in Medicine report 204 [18] with SSDE = conversion factor eff$_{dia}$ × CTDI$_{vol}$.

Fig. 2 Images of a representative patient from group 1 demonstrating **a** the line across which the signal intensity curves were generated in the left main artery and the full width at half maximum (FWHM) was calculated. Note the progressively increasing vessel sharpness from FBP. The parts of the profile curve below zero reflect the epicardial fat. Among the different ADMIRE strength levels 1 to 4, the highest vessel sharpness is eventually reached at a strength level of 5 in the signal profile (**b**)

The antero-posterior and lateral diameter for the calculations were measured by one reader in a mid-slice of the data set.

Statistical analysis

Quantitative variables were expressed as mean ± standard deviation and categorical variables as frequencies or percentages. The inter-reader agreement regarding qualitative evaluation was analysed by calculating weighted kappa statistics. Pearson's correlation coefficients were used to test for the interobserver agreement of the noise and contrast attenuation measurements. The Wilcoxon signed-rank test was used to test for significant differences in quantitative variables (including the FWHM) and the McNemar chi-square test for statistical comparison of categorical variables. A two-tailed p value less than 0.05 was considered to indicate statistically

Table 2 Qualitative and quantitative image quality in data sets reconstructed with FBP and with ADMIRE at strength levels of 1 to 5

	Group 1						Group 2
	FBP	ADMIRE 1	ADMIRE 2	ADMIRE 3	ADMIRE 4	ADMIRE 5	ADMIRE 4
IR-related image quality							
Excellent image quality (score 1)	–	84 % (21/25)	76 % (19/25)	56 % (14/25)	36 % (9/25)	12 % (3/25)	40 % (10/25)
Good image quality (score 2)	–	16 % (4/25)	24 % (6/25)	40 % (10/25)	56 % (14/25)	60 % (15/25)	48 % (12/25)
Fair image quality (score 3)	–	–	–	4 % (1/25)	8 % (2/25)	28 % (7/25)	12 % (3/25)
Poor image quality (score 4)	–	–	–	–	–	–	–
Graininess							
Excellent image quality (score 1)	–	–	–	–	80 % (20/25)	96 % (24/25)	72 % (18/25)
Good image quality (score 2)	–	–	36 % (9/25)	88 % (22/25)	20 % (5/25)	4 % (1/25)	28 % (7/25)
Fair image quality (score 3)	16 % (4/25)	56 % (14/25)	52 % (13/25)	12 % (3/25)	–	–	–
Poor image quality (score 4)	84 % (21/25)	44 % (11/25)	12 % (3/25)	–	–	–	–
Streak artefacts							
Score 1	88 % (22/25)	92 % (23/25)	96 % (24/25)	92 % (23/25)	92 % (23/25)	92 % (23/25)	96 % (24/25)
Score 2	12 % (3/25)	8 % (2/25)	4 % (1/25)	8 % (2/25)	8 % (2/25)	8 % (2/25)	4 % (1/25)
Score 3	–	–	–	–	–	–	–
Attenuation (range) [HU]	464±149 (308–744)	473±148 (312–755)	483±147 (309–755)	478±146 (306–755)	480±145 (307–755)	485±142 (307–756)	538±141 (344–757)
Image noise (range) [HU]	57±10 (35–72)	49±10 (30–64)	44±10 (27–59)	39±9 (24–54)	33±7 (20–45)	28±6 (16–39)	39±8 (29–50)
CNR (range)	11±4 (7–24)	13±5 (7–25)	15±5 (7–26)	17±6 (7–31)	20±8 (8–40)	23±8 (9–40)	16±5 (8–26)
FWMH [mm] in the LMA	5.7±2.0 (3.6–6.8)	5.1±1.3 (3.6–6.7)	5.0±1.2 (3.5–6.5)	4.9±1.3 (3.5–6.4)	4.8±1.3 (3.3–6.4)	4.6±1.4 (3.1–6.5)	–
FWMH [mm] in the PDA	3.5±0.4 (2.7–4.0)	3.1±0.4 (2.7–3.8)	3.0±0.5 (2.3–3.5)	2.8±0.5 (2.1–3.4)	2.7±0.5 (2.0–3.2)	2.6±0.5 (2.0–3.1)	–

FBP filtered back projection, *ADMIRE* advanced modelled iterative reconstruction, *IR* iterative reconstruction, *HU* Hounsfield units, *CNR* contrast-to-noise ratio, *FWHM* full width at half maximum of the signal intensity profile, *LMA* left main artery, *PDA* posterior descending artery

significant differences. All statistical analysis was conducted using IBM SPSS Statistics (release 21, Chicago, IL, USA).

Results

High-pitch CCTA was successfully performed in all 50 patients. Demographic parameters were not significantly different between groups (Table 1).

Patients had an average heart rate of 60±6 bpm (49–67 bpm). The average scan duration for CCTA was 158±10 ms (138–171 ms). In group 1, the automated tube voltage selection algorithm selected 70 kVp in one patient, 80 kVp in nine patients, 90 kVp in five patients, 100 kVp in four patients and 120 kVp in one patient; whereas in group 2, 70 kVp was selected in five patients, 80 kVp in seven patients and 90 kVp in eight patients. There was no significant difference in HR and tube voltage between groups (see Table 1).

Substantial coronary stenoses were present in three patients involving seven coronary segments in group 1 (12 %), and in four patients involving nine coronary segments in group 2

(16 %). Catheter coronary angiography was performed in these seven patients and confirmed the stenoses in all these 16 segments (100 %).

Qualitative image quality

None of the CCTA data sets were considered as being of non-diagnostic image quality by both readers. The inter-reader agreement was considered excellent (kappa=0.81). Thus, the qualitative evaluation of reader 1 was used for further analysis.

A total of 347 coronary artery segments were evaluated in group 1 and a total of 351 coronary artery segments in group 2. The weakest IR-related image appearance was found with ADMIRE strength level 1 (84 %, 21/25 with an excellent image quality) with only minor degradation at lower ADMIRE strength levels. The strongest IR-related image appearance was obtained with ADMIRE strength level 5 with 12 % (3/25) having an excellent image quality, 60 % (15/25) having a good image quality and 28 % (7/25) having a fair image quality (Table 2).

Fig. 3 Box plots indicating quantitative image noise (**a**) and CNR (**b**) in the ascending aorta in group 1 in images reconstructed with FBP and with ADMIRE at strength levels from 1 to 5, and in group 2 in images reconstructed with ADMIRE at a strength level of 4. *Box* first to third quartiles; *bold line* median; *whiskers* the lowest datum still within 1.5 interquartile range of the lower quartile, and the highest datum still within 1.5 interquartile range of the upper quartile; ○ outlier
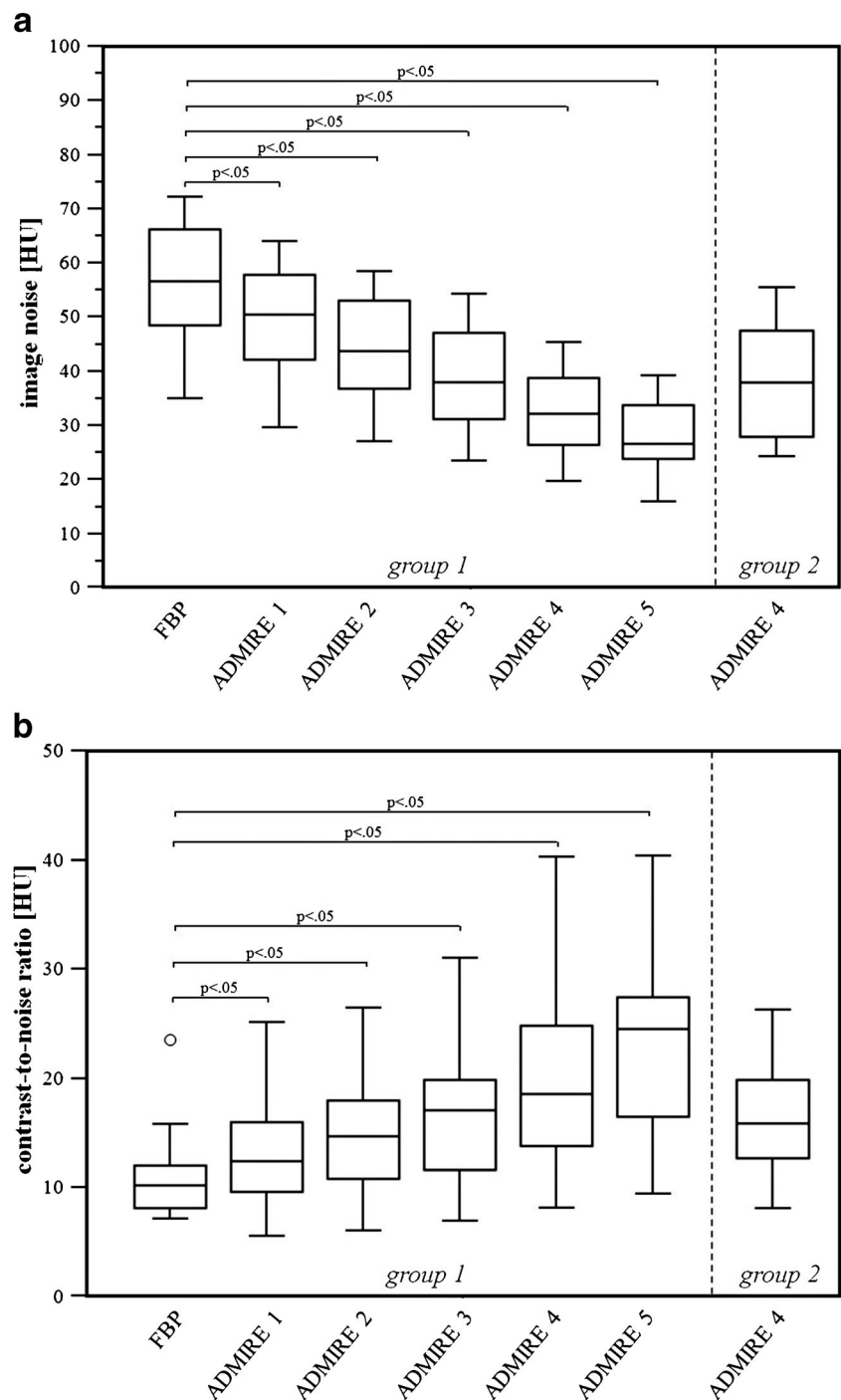
Graininess score was worst in FBP (84 % of poor image quality) and was highest when using ADMIRE at a strength level of 5 in group 1 (96 % of excellent image quality regarding graininess; Table 2).

Streak artefacts were only occasionally found in the presence of severely calcified coronary artery plaques. There was no substantial difference in the presence of streak artefacts among the different reconstruction methods and groups. In addition, no streak artefacts were considered to interfere with the depiction of adjacent structures (score 3; Table 2).

The ADMIRE strength level 4 was most often selected (84 %, 21/25) by the two readers as the preferred data set for making the diagnosis, followed by ADMIRE strength 3 (12 %, 3/25) and ADMIRE strength 5 (4 %, 1/25). Given that

the standard institutional high-pitch CCTA protocol was intended for FBP reconstructions, we used the percentage of noise reduction at ADMIRE strength 4 in comparison to FBP for selecting the corresponding reduction of the reference tube current in group 2.

In group 2, the IR-related image appearance and graininess scores with a reduced reference tube current and ADMIRE 4 reconstruction were comparable to that of group 1 with ADMIRE 3 and ADMIRE 4, respectively.

Image sharpness evaluation

The vessel sharpness according to the signal intensity profiles in all 10 patients from group 1 was lowest in data sets reconstructed with FBP and highest in those reconstructed with ADMIRE 5, in both proximal and distal vessels (Fig. 2).

ADMIRE images at any strength level demonstrated a significantly lower FWHM in the LMA and in the PDA than images reconstructed with FBP ($p<0.05$; Table 2). Among the five strength levels of ADMIRE, there was no significant difference in FWHM; however, a non-significant tendency towards a lower FWHM at higher strength levels was noted.

Quantitative image quality

The interobserver agreements were excellent for measurements of the attenuation (mean difference 26 ± 12 HU, $r=0.88$, $p<0.01$) and image noise (mean difference 6 ± 3 HU, $r=0.85$, $p<0.01$). Therefore, the average of measurements from both readers was used for further analysis.

In group 1, there was a significant decrease of image noise with each ADMIRE strength level increase and in comparison to FBP ($p<0.05$) and, in distinction, a significant increase in

CNR with each ADMIRE level increase and in comparison to FBP ($p<0.05$; Table 2; Fig. 3a, b). There was no significant difference in attenuation among the ADMIRE levels and FBP ($p=NS$). The noise reduction at ADMIRE level 4 compared to FBP was 42 %. Consequently, the reference tube current–time product for group 2 was reduced to 160 mAs/rot.

In group 2, the average image noise was 39 ± 8 HU and the CNR was 16 ± 5, comparable to the quantitative image quality parameters using ADMIRE level 2–3 in group 1 (Fig. 3). None of the CCTA examinations in group 2 were of non-diagnostic image quality (Fig. 4).

Radiation dose

The average radiation dose of CCTA in group 1 was 0.5 ± 0.3 mSv, being significantly higher than the estimated effective radiation dose in group 2 (0.3 ± 0.1 mSv; $p<0.05$; Table 1). Similarly, SSDE was significantly higher in group 1 compared to group 2 (1.9 ± 1.0 mGy vs. 1.4 ± 0.4 mGy, $p<0.05$).

Discussion

IR techniques are being increasingly used in CCTA because they provide the potential for lowering radiation dose [19–23]. For CCTA, the application of IR also has beneficial effects for reducing blooming artefacts from severely calcified plaques and stents [24, 25].

With early-generation IR techniques, CT images often were reported to appear pixelated and plastic-like, resulting in an unfamiliar appearance. Vendors have addressed this issue by providing adjustable parameters influencing the level of noise reduction and edge enhancement, blending with FBP
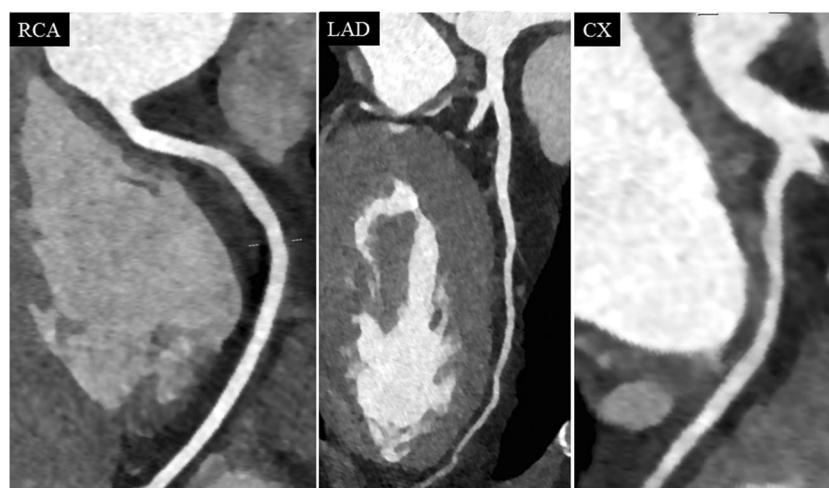

Fig. 4 CCTA study of a 58-year-old man with atypical chest pain having a low risk of coronary artery disease from group 2. Heart rate was 72 bpm and BMI was 26.8 kg/m². CCTA was performed at an effective tube voltage of 90 kVp and an effective tube current–time product of 222 mAs/rot. Images reconstructed with ADMIRE strength level 4 demonstrate good to excellent image quality of the right coronary artery (*RCA*), the left anterior descending artery (*LAD*), and circumflex artery (*CX*). Image noise in the ascending aorta was 30 HU; the CNR was 16

algorithms, selection of strength levels and by developing algorithms associated to a lesser degree with such appearances [14]. The IR technique applied in this study represents the third-generation approach of one vendor, which was also aimed at a reduction of the plastic-like image appearance at higher strength levels.

We aimed to determine the dose reduction potential of this IR algorithm in low radiation dose CCTA. In the first part of the study, ADMIRE at all levels was applied to a protocol with prospectively ECG-gated high-pitch spiral acquisition and automated tube voltage selection, being associated with an average effective dose of 0.5 mSv. Increasing the strength level in ADMIRE yielded a stepwise improvement in quantitative image quality in terms of noise and CNR. Furthermore, vessel sharpness was increased at higher as compared to lower levels and to FBP, as demonstrated in the FWHM analysis. In addition, we observed that both experienced readers preferred the ADMIRE data set at a level of 4 for reading the images and for making the diagnosis. This slight mismatch between quantitative (i.e. noise and FWHM analysis showing best results at strength level 5) and qualitative image quality (i.e. preferred data set selection at level 4) is a phenomenon which is known from previous studies employing IR [26]. Overall, we used the results obtained at an ADMIRE strength level 4 as those for translation into the second part of the study, where the use of IR was applied for reducing the radiation dose of the CCTA examinations to a level being as low as 0.3 mSv.

In a recent study, Schuhbaeck et al. [21] showed that the application of second-generation IR in combination with high-pitch spiral acquisition may allow for CCTA at an effective dose below 0.1 mSv. However, that study included only normal-weight patients, whereas we included patients irrespective of their body weight and/or BMI. Moreover, the average image noise in the previous study [21] (129 HU) was considerably higher than that encountered in this study (ranging between 28–49 HU).

Interestingly, the reduction of the reference tube current resulted in a trend, albeit non-significant, towards automatically selected lower voltages in group 2. At a reference tube voltage of 100 kVp in group 1, 5/25 patients were scanned with 100 kVp or higher. In distinction, none of the patients from group 2 (using the same reference tube voltage but a lower reference tube current) were scanned with 100 kVp or higher. This indicates the inter-relationship between tube current and voltage: The reference tube current determines the desired image quality and the automated attenuation-based tube potential selection determines the optimal combination of tube voltage and current for the individual body region and the respective indication [27].

Some study limitations must be acknowledged. First, we included a relatively small patient cohort. Second, we investigated the performance of latest-generation IR of a single vendor only; thus, transfer of results to CT scanners from other vendors is limited. Third, although all images were anonymized, the obvious differences in image appearance between reconstruction methods precludes observer blinding, thus resulting in potential bias. Fourth, the assessment of quantitative noise in IR images is known to be inaccurate when using the parameter standard deviation of the attenuation, because noise is known to be unequally distributed in IR images. However, this still provides some estimation of noise, and additional quantitative parameters such as the FWHM of the vessel contour sharpness were included in this study. Fifth, we did not control for coexisting cardiac disease potentially leading to a change in attenuation and CNR. However, patients in this study had a low to intermediate risk of coronary artery disease, so the risk of including patients with alterations in cardiac output was low. Sixth, it is known that changes in tube voltage can influence qualitative and quantitative image quality. However, the purpose of this study was not a comparison of two differently scanned patient populations but rather to demonstrate the effect of using ADMIRE in high-pitch CCTA in one patient population, with the results of this evaluation being translated to a reduction in radiation dose in another patient group. Finally, reduction of radiation dose by using IR of 0.2 mSv per examination could be considered negligible. However, given the widespread and continuously increasing application of cardiac CT together with the current belief that no threshold exists for the cancer risk from ionizing radiation, every effort must be undertaken for reducing the radiation dose according to the ALARA principle.

In conclusion, this study shows that IR can be used for optimizing and lowering the radiation dose of 192-slice dual-source CCTA in the high-pitch mode, being associated with a diagnostic image quality at a radiation of 0.3 mSv.

References

1. Tamm EP, Rong XJ, Cody DD, Ernst RD, Fitzgerald NE, Kundra V (2011) Quality initiatives: CT radiation dose reduction: how to implement change without sacrificing diagnostic quality. Radiographics 31:1823–1832

2. Layritz C, Muschiol G, Flohr T et al (2013) Automated attenuation-based selection of tube voltage and tube current for coronary CT angiography: reduction of radiation exposure versus a BMI-based

strategy with an expert investigator. J Cardiovasc Comput Tomogr 7:303–310

3. Vardhanabhuti V, Riordan RD, Mitchell GR, Hyde C, Roobottom CA (2014) Image comparative assessment using iterative reconstructions: clinical comparison of low-dose abdominal/pelvic computed tomography between adaptive statistical, model-based iterative reconstructions and traditional filtered back projection in 65 patients. Invest Radiol 49:209–216

4. Meyer M, Haubenreisser H, Schoepf UJ et al (2014) Closing in on the K edge: coronary CT angiography at 100, 80, and 70 kV-initial comparison of a second- versus a third-generation dual-source CT system. Radiology. doi:10.1148/radiol.14140244:140244

5. Morsbach F, Gordic S, Desbiolles L et al (2014) Performance of turbo high-pitch dual-source CT for coronary CT angiography: first ex vivo and patient experience. Eur Radiol 24:1889–1895

6. Gordic S, Husarik DB, Desbiolles L, Leschka S, Frauenfelder T, Alkadhi H (2014) High-pitch coronary CT angiography with third generation dual-source CT: limits of heart rate. Int J Cardiovasc Imaging 30:1173–1179

7. Gordic S, Morsbach F, Schmidt B et al (2014) Ultralow-dose chest computed tomography for pulmonary nodule detection: first performance evaluation of single energy scanning with spectral shaping. Invest Radiol 49:465–473

8. Gordic S, Desbiolles L, Stolzmann P et al (2014) Advanced modelled iterative reconstruction for abdominal CT: qualitative and quantitative evaluation. Clin Radiol 69:e497–e504

9. Pontana F, Pagniez J, Flohr T et al (2011) Chest computed tomography using iterative reconstruction vs filtered back projection (Part 1): evaluation of image noise reduction in 32 patients. Eur Radiol 21:627–635

10. Thibault JB, Sauer KD, Bouman CA, Hsieh J (2007) A three-dimensional statistical approach to improved image quality for multislice helical CT. Med Phys 34:4526–4544

11. Taylor AJ, Cerqueira M, Hodgson JM et al (2010) ACCF/SCCT/ACR/AHA/ASE/ASNC/NASCI/SCAI/SCMR 2010 appropriate use criteria for cardiac computed tomography. A report of the American College of Cardiology Foundation Appropriate Use Criteria Task Force, the Society of Cardiovascular Computed Tomography, the American College of Radiology, the American Heart Association, the American Society of Echocardiography, the American Society of Nuclear Cardiology, the North American Society for Cardiovascular Imaging, the Society for Cardiovascular Angiography and Interventions, and the Society for Cardiovascular Magnetic Resonance. Circulation 122:e525–e555

12. Pontana F, Duhamel A, Pagniez J et al (2011) Chest computed tomography using iterative reconstruction vs filtered back projection (Part 2): image quality of low-dose CT examinations in 80 patients. Eur Radiol 21:636–643

13. Morsbach F, Desbiolles L, Plass A et al (2013) Stenosis quantification in coronary CT angiography: impact of an integrated circuit detector with iterative reconstruction. Invest Radiol 48:32–40

14. Wang R, Schoepf UJ, Wu R et al (2014) Diagnostic accuracy of coronary CT angiography: comparison of filtered back projection and iterative reconstruction with different strengths. J Comput Assist Tomogr 38:179–184

15. Richard S, Husarik DB, Yadava G, Murphy SN, Samei E (2012) Towards task-based assessment of CT performance: system and object MTF across different reconstruction algorithms. Med Phys 39:4115–4122

16. Menzel HG, Schibilla H, Teunen D (eds) (2000) European guidelines on quality criteria for computed tomography, EUR 16262 EN. European Commission, Luxembourg

17. Einstein AJ, Elliston CD, Arai AE et al (2010) Radiation dose from single-heartbeat coronary CT angiography performed with a 320-detector row volume scanner. Radiology 254:698–706

18. Boone JM, Strauus KJ, Cody DD, McCollough CH, McNitt-Gray MF, Toth TL (2011) Size specific dose estimates (SSDE) in pediatric and adult CT examinations. American Association of Physicists in Medicine, report of AAPM Task Group 204. AAPM, College Park, MD

19. Hou Y, Liu X, Xv S, Guo W, Guo Q (2012) Comparisons of image quality and radiation dose between iterative reconstruction and filtered back projection reconstruction algorithms in 256-MDCT coronary angiography. AJR Am J Roentgenol 199:588–594

20. Leipsic J, Labounty TM, Heilbron B et al (2010) Adaptive statistical iterative reconstruction: assessment of image noise and image quality in coronary CT angiography. AJR Am J Roentgenol 195:649–654

21. Schuhbaeck A, Achenbach S, Layritz C et al (2013) Image quality of ultra-low radiation exposure coronary CT angiography with an effective dose <0.1 mSv using high-pitch spiral acquisition and raw data-based iterative reconstruction. Eur Radiol 23:597–606

22. Singh S, Khawaja RD, Pourjabbar S, Padole A, Lira D, Kalra MK (2013) Iterative image reconstruction and its role in cardiothoracic computed tomography. J Thorac Imaging 28:355–367

23. Yin WH, Lu B, Hou ZH et al (2013) Detection of coronary artery stenosis with sub-milliSievert radiation dose by prospectively ECG-triggered high-pitch spiral CT angiography and iterative reconstruction. Eur Radiol 23:2927–2933

24. Ebersberger U, Tricarico F, Schoepf UJ et al (2013) CT evaluation of coronary artery stents with iterative image reconstruction: improvements in image quality and potential for radiation dose reduction. Eur Radiol 23:125–132

25. Renker M, Nance JW Jr, Schoepf UJ et al (2011) Evaluation of heavily calcified vessels with coronary CT angiography: comparison of iterative and filtered back projection image reconstruction. Radiology 260:390–399

26. Husarik DB, Schindera ST, Morsbach F et al (2014) Combining automated attenuation-based tube voltage selection and iterative reconstruction: a liver phantom study. Eur Radiol 24:657–667

27. Winklehner A, Goetti R, Baumueller S et al (2011) Automated attenuation-based tube potential selection for thoracoabdominal computed tomography angiography: improved dose effectiveness. Invest Radiol 46:767–773